

I. DERÉNYI

Application of the ratchet effect to improve material quality (reducing vortex density in superconductors and smoothing surfaces)

Institut Curie, UMR 168, 26 rue d'Ulm, 75248 Paris Cédex 05, France

Received: 20 November 2001 / Accepted: 14 January 2002
 Published online: 22 April 2002 • © Springer-Verlag 2002

ABSTRACT Although Brownian ratchets have been conceived to describe the operation of molecular motor proteins, their basic principles are also applicable to a wide range of different physical systems. In this paper I line up two such possible applications in condensed-matter physics. The first one is the removal of vortices from superconductors. Magnetic fields frequently penetrate superconducting materials in the form of vortices, and once present, they dissipate energy and generate internal noise, limiting the operation of numerous superconducting devices. We demonstrate theoretically that the application of an alternating current to a superconductor patterned with an appropriate ratchet-like pinning potential induces an outward vortex motion. The second application is based on the fact that the Schwoebel barrier induces an asymmetry in the lattice potential of nearly flat solid surfaces. During epitaxial growth this asymmetry leads to a fast and unwanted increase in the surface roughness. We show, however, that one can take advantage of the asymmetry by applying an alternating electric field parallel to the surface, which induces a net electromigrational flow of the surface atoms from the peaks towards the wells, and thus results in a smoother surface.

PACS 05.40.-a; 68.35.-p; 74.60.Ge

1 Vortex removal from superconductors

A serious obstacle impeding the application of low- and high-temperature superconductor devices is the presence of trapped magnetic flux [1–4]. Flux lines or vortices can be induced by fields as small as the Earth's magnetic field. Once present, vortices dissipate energy and generate internal noise. Methods used to overcome these difficulties include the pinning of vortices by the incorporation of impurities and defects [5], the construction of flux dams [6], slots and holes [7], the application of high-frequency magnetic fields [8], and the application of magnetic shields [2–4], which block the penetration of new flux lines in the bulk of the superconductor or reduce the magnetic field in the immediate vicinity of the superconducting device. The most desirable method would be to remove the vortices from the bulk of the superconductor,

but there was hitherto no known phenomenon that could form the basis for such a process. Here I show that the application of an alternating current to a superconductor patterned with an asymmetric pinning potential can induce vortex motion whose direction is determined only by the asymmetry of the pattern [9]. The mechanism responsible for this phenomenon is the so-called ratchet effect [10–18], and its working principle applies to both low- and high-temperature superconductors. I demonstrate theoretically that, with an appropriate choice of the pinning potential, the ratchet effect can be used to remove vortices from low-temperature superconductors.

Consider a type-II superconductor film of the geometry shown in Fig. 1, placed in an external magnetic field, H . The superconductor is patterned with a pinning potential $U(x, y) = U(x)$, which is periodic with period ℓ along the x -direction, has an asymmetric shape within one period, and is translationally invariant along the y -direction of the sample.

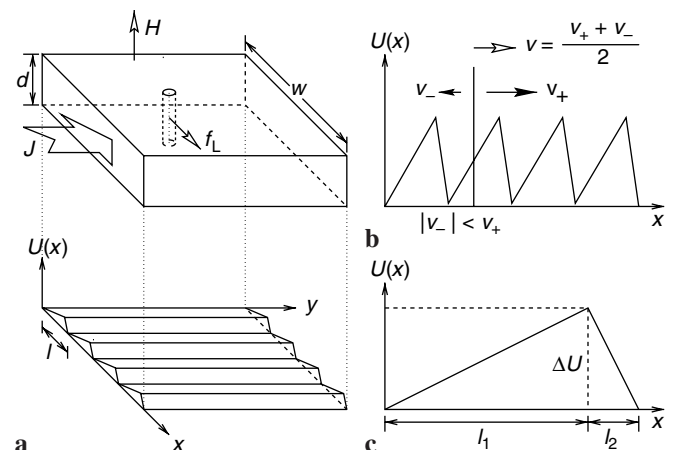


FIGURE 1 a Diagram of a superconductor in the presence of an external magnetic field, H . A dc current with density J flowing along the y -direction (large arrow) induces a Lorentz force, f_L , that moves the vortex in the x -direction. The superconductor is patterned with a pinning potential $U(x, y) = U(x)$, whose shape is shown in the lower panel. The potential is periodic and asymmetric along the x -direction, and is translationally invariant along the y -direction. b The pinning potential, $U(x)$, along the superconductor's cross-section. The solid arrows indicate the vortex velocity v_+ (v_-) induced by a direct $+J$ (reversed $-J$) current. The average, $v = (v_+ + v_-)/2$, is the ratchet velocity of the vortex, obtained when an ac current is applied. c The definition of the parameters characterizing a single tooth of the asymmetric potential

The simplest example of an asymmetric periodic potential is the asymmetric sawtooth potential, shown in Fig. 1b. Because the vortex line energy is linearly proportional to the thickness of the sample, such a potential can be obtained by varying the sample thickness. Similar potentials can also be obtained by creating point defects in the sample with sawtooth-like distributions [19] or with pinning strengths that vary in an asymmetric fashion [20]. In the presence of a current with density \mathbf{J} flowing along the y -axis, the vortices move with the velocity $\mathbf{v} = (\mathbf{f}_L + \mathbf{f}_{vv} + \mathbf{f}_u)/\eta$, where $\mathbf{f}_L = (\mathbf{J} \times \hat{\mathbf{h}})\Phi_0 d/c$ is the Lorentz force moving the vortices transverse to the current, c is the speed of light in vacuum, $\hat{\mathbf{h}}$ is the unit vector pointing in the direction of the external magnetic field \mathbf{H} , $\mathbf{f}_u = -\frac{dU}{dx}\hat{\mathbf{x}}$ is the force generated by the periodic potential, \mathbf{f}_{vv} is the repulsive vortex–vortex interaction, $\Phi_0 = 2.07 \times 10^{-7} \text{ G cm}^{-2}$ is the flux quantum, η is the viscous drag coefficient, and d is the length of the vortices (i.e. the thickness of the sample).

When a direct current flows along the positive y -direction, the Lorentz force moves the vortices along the positive x -direction with velocity v_+ . Reversing the current reverses the direction of the vortex velocity, but its magnitude, $|v_-|$, due to the asymmetry of the potential, is different from v_+ . This is a well-known property of the so-called rocking ratchets [11]. For the sawtooth potential shown in Fig. 1b the vortex velocity is higher when the vortex is driven to the right than when it is driven to the left ($v_+ > |v_-|$). As a consequence the application of an alternating (square wave) current results in a net velocity $v = (v_+ + v_-)/2$ to the right in Fig. 1b. This net velocity induced by the combination of an asymmetric potential and an alternating driving force is called the ratchet velocity [10–18]. The ratchet velocity for low vortex density (when vortex–vortex interactions are neglected) can be calculated analytically. For an increasing period, T , it converges to [9]

$$v = \begin{cases} 0 & \text{if } f_L < f_1, \\ \frac{1}{2\eta} \frac{(f_1 + f_2)(f_1 - f_1)}{f_1 + f_2 - f_1} & \text{if } f_1 < f_L < f_2, \\ \frac{1}{\eta} \frac{f_1 f_2 (f_2 - f_1)}{f_L^2 - (f_2 - f_1)^2} & \text{if } f_2 < f_L, \end{cases} \quad (1)$$

where $f_1 = \Delta U/\ell_1$ and $f_2 = \Delta U/\ell_2$ are the magnitudes of the forces generated by the ratchet potential on the facets of length ℓ_1 and ℓ_2 , respectively (see Fig. 1c), ΔU is the energy difference between the maximum and the minimum of the potential, and $f_L = |\mathbf{f}_L| = J\Phi_0 d/c$.

A similar mechanism is responsible for the asymmetric dynamics of vortices near surface steps [21, 22]. The steps act as vortex diodes, impeding the motion from the thinner to the thicker part of the sample, while leaving the motion in the opposite direction unaffected.

Molecular-dynamics simulations [9], using the model developed by Nori and collaborators [23–25], confirm that, as long as the average separation between the vortices along the potential wells is large compared to the penetration depth, λ ($\approx 45 \text{ nm}$ for Nb), the speed of the vortices is in good agreement with the analytic formula (1). However, for increasing vortex density, the average separation decreases and the vortices start to pile up and smoothen the ratchet potential, which then leads to a decreasing ratchet velocity. For a thin Nb film ($d \approx 5\lambda$, $\ell_1 \approx 20\lambda$, $\ell_2 \approx 5\lambda$, and pattern height $\Delta h \approx 5\lambda$) the typical force scale is 10^{-11} N , ΔU is about $4 \times 10^{-18} \text{ J}$, and

the maximum ratchet velocity is around 5 m s^{-1} , which is fast enough to move a vortex across a typical, few-micrometer-wide sample [3] within a few microseconds.

Next, we discuss a potentially useful application of the ratchet effect by demonstrating that it could be used to drive vortices out of a superconductor. Consider a superconductor film that is patterned with two arrays of the ratchet potential oriented in opposite directions, as shown in Fig. 2a. During

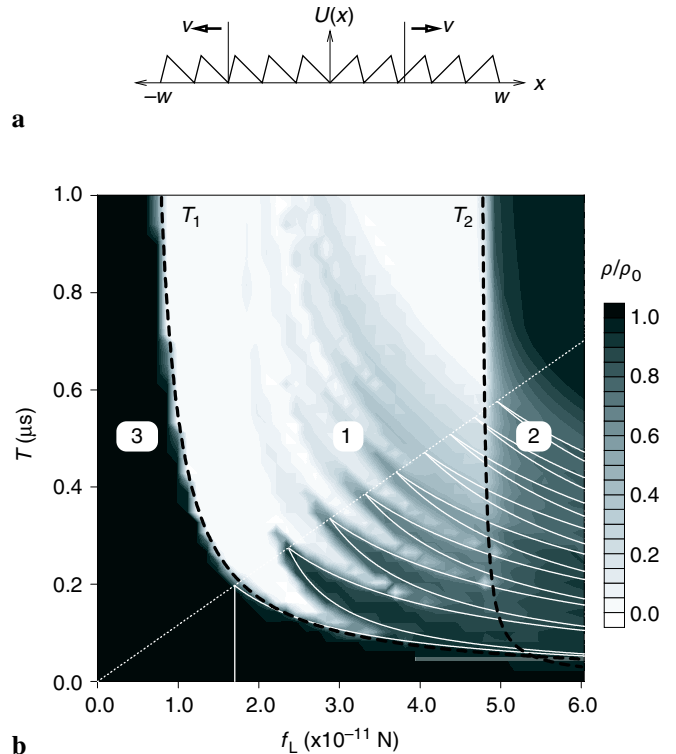


FIGURE 2 **a** Two ratchet potentials oriented in opposite directions, leading to an outward vortex motion. **b** The remaining vortex density, ρ , after vortex removal plotted on the (f_L, T) parameter plane. The gray scale corresponds to the relative vortex density, ρ/ρ_0 , where ρ_0 is the initial density corresponding to a magnetic field of $H = 1 \text{ G}$. The parameters of each tooth used in the molecular dynamics simulations are: $d = 5\lambda$, $\ell_1 = 20\lambda$, $\ell_2 = 5\lambda$, and pattern height $\Delta h = 5\lambda$. For Nb the penetration depth is $\lambda \approx 45 \text{ nm}$, the vortex line energy per unit length is $\varepsilon_0 \approx 1.7 \times 10^{-11} \text{ J m}^{-1}$, and the viscosity per unit length is $\eta_0 \approx 7 \times 10^{-6} \text{ N s m}^{-2}$. To mimic the pressure generated by the external magnetic field, which acts to push vortices into the sample, we attached a reservoir with constant vortex density, ρ_0 , to each side. In thin superconducting films, due to the Meissner current, there is a geometrical barrier that acts to trap the vortices inside the sample [26]. As most applications of superconductors involve thin films, we included this geometrical barrier in the simulations, which creates the force $f_{in}(x) = -\frac{H\Phi_0}{2\pi} x/\sqrt{w^2 - x^2}$ for $-w + d/2 < x < w - d/2$, and $f_{edge} = 2\varepsilon_0 - \frac{H\Phi_0}{2\pi} \sqrt{4w/d - 1}$ for $x > w - d/2$, and $-f_{edge}$ for $x < -w + d/2$. Thus the geometrical barrier opposes the entry of the vortices at the edge of the superconductor, but once they move inside, it moves them towards the center of the superconductor. For successful vortex removal, the ratchet effect has to be strong enough to move the vortices against $f_{in}(x)$. The analytically calculated dashed black lines, $T_1(f_L)$ (the time needed for a vortex to move all the way up on the long facet of the last tooth) and $T_2(f_L)$ (the time needed to enter from the edge over the first potential maximum), separate the three main regimes: regime 1, where the vortex removal is complete almost everywhere; regime 2, with partial vortex removal; and regime 3, with no change in the vortex density. The thin white solid lines denote the boundaries of the regions where vortex trapping occurs due to periodic orbits. These boundaries correctly reflect the structure of the fingers, but slightly deviate from the results of the simulation, because the analytical calculation assumed an infinite array of identical teeth

the application of the ac current, the asymmetry of the potential in the right half moves the vortices in that region to the right, while vortices in the left half move to the left. Thus the vortices drift towards the closest edge of the sample, decreasing the vortex density in the bulk of the film.

We performed numerical simulations to quantitatively characterize this effect (details and parameters are described in the legend of Fig. 2). For simplicity, the dependence of the Lorentz force, f_L , and of the viscous drag coefficient, η , on the film thickness was neglected. In Fig. 2b we summarize the effectiveness of vortex removal by plotting the reduced vortex density inside the film as a function of f_L and the period, T , of the current. There is a well-defined region where the vortex density drops to zero inside the sample, indicating that the vortices are completely removed. Outside this region we observe either a partial removal or the ac current has no effect on the vortex density. The (f_L, T) diagram in Fig. 2b has three main regimes (1, 2 and 3) separated by two boundaries [9]. The $T_1(f_L)$ phase boundary provides the time needed to move the vortex all the way up on the ℓ_1 long facet of the ratchet potential at the edge of the superconductor, i.e. to remove the vortex from the superconductor. When $T < T_1$ the vortices cannot leave the superconductor. The T_2 phase boundary is the time needed for a vortex to enter from the edge of the superconductor past the first potential maximum. Thus, when $T < T_2$ the vortices cannot overcome the edge of the potential barrier. These phase boundaries (calculated for non-interacting vortices) effectively determine the vortex density in the three regimes. Vortex removal is most effective in regime 1, where the vortices cannot move past the first potential barrier when they try to enter the superconductor, but they get past the barriers opposing their exit from it. Thus the vortices are swept out of the superconductor by the ratchet effect, and no vortex can re-enter, leading to zero vortex density. Indeed, the numerical simulations indicate complete vortex removal in much of this regime. An exception is the finger structure near the crossing of the T_1 and T_2 boundaries. For fields and periods within the first finger (situated almost entirely in regime 3 in Fig. 2b), the vortex follows a periodic orbit inside a single potential well [17]. The subsequent fingers represent stable periodic orbits between two, three, or more wells, respectively. As the vortices cannot escape from these orbits, they remain trapped inside the superconductor, increasing the vortex density within the fingers in the phase diagram. Figure 2b shows (as white solid lines) the analytically calculated envelopes of the regions where such trapping occurs. An important feature of the finger structure is that stable periodic orbits do not exist above the line $T_{\text{tip}} = f_L \frac{2\eta\Delta U}{f_1 f_2 (f_2 - f_1)}$ connecting the finger tips. In regime 2 vortices can enter the superconductor, but the ratchet effect is still sweeping them out; so here we expect partial removal of the vortices, the final vortex density inside the superconductor being determined by the balance of vortex nucleation rate at the edge of the sample (which depends on its surface properties) and the ratchet velocity moving them out. In regime 3 the vortices cannot leave the superconductor and new vortices cannot enter the system; thus the initial density inside the superconductor is unchanged throughout this regime.

The positions of the phase boundaries T_1 and T_2 depend on the shape of sample and on the external magnetic field. For large fields regime 1 can disappear. However, for samples with elliptic cross-section the geometric barrier (described in Fig. 2) can be eliminated [27]; thus regime 1 with complete vortex removal could be extended to high magnetic fields as well.

Vortex removal is important for numerous applications of superconductors and can improve the functioning of several devices. An immediate application of the proposed method would be to improve the operation of superconducting quantum interference devices (SQUIDs), used as sensors in a wide assortment of scientific instruments [3, 28, 29]. A long-standing issue in the performance of SQUIDs is $1/f$ noise [7, 28], arising from the activated hopping of trapped vortices [1]. Reduction of the vortex density in these superconductors is expected to extend the operation regime of these devices to lower frequencies.

Although over the past few years several applications of the ratchet effect have been proposed, such as separating particles [30, 31], designing molecular motors [32, 33], smoothing surfaces [34], or rectifying voltage in Josephson junctions [35–41], our proposal solves an acute problem of condensed-matter physics, by removing vortices from a superconductor. In contrast with most previous applications, which require the presence of thermal noise, this model is completely deterministic. Indeed, in Nb the variation in the pinning potential is $\Delta U \approx 25$ eV, which is more than 10^4 times larger than $k_B T \approx 0.8$ meV at $T_c = 9.26$ K, thus rendering thermal fluctuations irrelevant. A particularly attractive practical feature of our proposed method is that it does not require sophisticated material processing to make it work. First, it requires standard, micrometer-scale patterning techniques (the micrometer tooth size was chosen so that a few teeth fit on a typical SQUID, but a larger feature size will also function if the period, T , is increased proportionally). Second, the application of an ac current with appropriate period and intensity is rather easy to achieve. For applications where an ac current is not desired, the vortices can be flushed out before normal operation of the device. On the other hand, if the superconducting device is driven by an ac current (e.g. radio-frequency SQUIDs, ac magnets, or wires carrying ac current), the elimination of the vortices will take place continuously during the operation of the device. The analytically predicted phase boundaries, whose position is determined by the geometry of the patterning, provide a useful tool for designing the appropriate patterning to obtain the lowest possible vortex density for the current and frequency ranges desired for specific applications. Although here we limited ourselves to low-temperature superconductors, the working principle of the ratchet effect applies to high-temperature superconductors as well.

Another kind of application of the ratchet effect in superconductors has recently been proposed by Wambaugh et al. [42]. Their approach is based on two-dimensional vortex channels [43] (where the pinning is very weak inside and very strong outside) with asymmetric channel walls (Fig. 3). These geometric ratchets [44–47], driven by alternating currents, could be used to transport, concentrate, and disperse vortices in nano-devices.

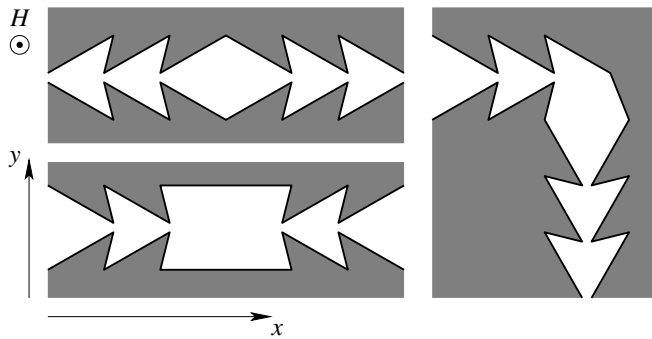


FIGURE 3 Schematic of vortex channels with ratchet-like walls. The pinning is weak inside (white part) and strong outside (gray part). The vortices and the magnetic field are parallel to the z -axis. An alternating current will drive the vortices out of the center in the upper left setup and towards the center in the lower left one. A current alternating in both the x - and y -directions can drive the vortices along the channel of the figure on the right

2 Surface smoothing with electromigration

Growing epitaxial films with smooth surfaces is one of the ongoing challenges of the thin-film community. However, this goal is hampered by a series of basic physical effects that lead to the development of unavoidable surface roughness during growth. In particular, there is abundant experimental and theoretical evidence that during deposition the diffusion bias generated by the Schwoebel barrier (see Fig. 4) results in a net uphill current, which in turn leads to the formation of mounds and to a fast and unwanted increase in the interface roughness [48–51]. As Fig. 4 demonstrates, the Schwoebel barrier introduces spatial asymmetry in the otherwise symmetric lattice potential. Surface atoms driven by an alternating electric field on such a potential experience the ratchet effect [10–18], which results in a net downhill migration, and thereby, smoothens the surface [34].

Atom diffusion on crystal surfaces is a thermally activated process: atoms can hop from their position to a neighboring one by overcoming a potential barrier, ΔE . The hopping rate is given by the Arrhenius law: $k = \nu_0 \exp(-\Delta E/k_B T)$, where T is the temperature and ν_0 is the vibration frequency of the surface atoms. Figure 4 illustrates the lattice potential of a vicinal surface that consists of long flat terraces separated by

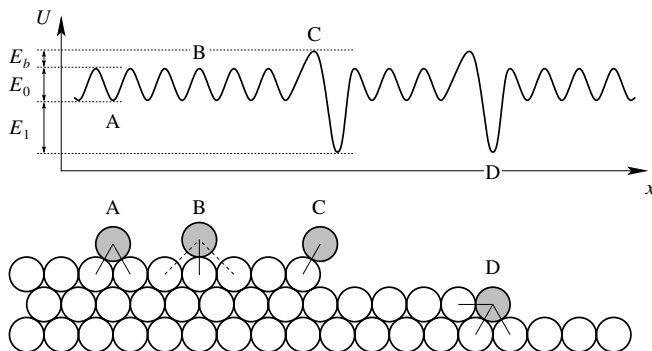


FIGURE 4 Schematic of the cross-section of a vicinal surface (lower panel) containing two monatomic steps and the asymmetric lattice potential (upper panel) experienced by the atoms (gray circles) diffusing on this surface. Note that a non-zero Schwoebel barrier, E_b , is necessary to break the spatial symmetry of the potential. A downhill current points to the right in this figure

monatomic steps. The barrier height for diffusion on a flat surface is denoted by E_0 . Near a step atoms form additional lateral bonds of energy, E_1 , with the step atoms, leading to a deeper potential valley. Finally, jumping over a step requires breaking several bonds, and therefore the diffusing atom must pass an additional potential barrier: the Schwoebel barrier, E_b [52, 53].

For most metals and semiconductors the otherwise random surface diffusion of the atoms can be biased by an external electric field applied parallel to the surface, a phenomenon known as surface electromigration [54–57]. The effective force, $F = ZeE$, acting on the surface atoms is proportional to the field E , where the coefficients e and Z are the elementary charge (> 0) and the effective charge number, respectively. The effective charge number consists of two terms, $Z = Z_d + Z_w$. The “direct” term, $Z_d (> 0)$, is associated with the electrostatic interaction between the atom and the electric field, while the “wind” term, $Z_w (< 0)$, is generated by the scattering of the current-carrying electrons on the surface atoms. The competition between these two terms can result in either a positive or a negative effective charge [58, 59].

Thus, a constant electric field induces a current in the surface atoms parallel to the field. Moreover, due to the asymmetry of the surface potential (caused by the non-zero Schwoebel barrier), an alternating electric field also generates a non-zero net current, as a manifestation of the ratchet effect. Because the Schwoebel barrier slows down the current to a greater extent when it flows in the ascending step direction, the induced net current is always downhill, i.e. it points towards the descending step direction, independent of the step orientation or the effective charge. Since the downhill current acts to smooth the surface, it has the potential to accelerate the smoothing process during annealing and to slow or eliminate the Schwoebel-barrier-induced mound formation during growth. Consequently, this nano-scale ratchet effect can have important technological applications for thin-film growth.

For a single atom moving on a fixed surface with uniform steps, the net current can be calculated analytically [34]. Although the calculation correctly describes the nature and the qualitative features of the net current, it neglects the atom-atom interaction [60] and the step fluctuations. Since the source of the atoms are the steps (adatoms detach from step edges), the step length is not fixed, but it fluctuates. To incorporate these effects we performed Monte Carlo simulations with activated diffusion along the surface.

As a demonstration of the smoothing of an initially rough morphology due to the ratchet effect, we investigated the evolution of the mound structure shown in Fig. 5a. Each mound has a triangular shape of base size 300 lattice constants and a height of 30, such that the sides of the triangular shapes are formed of steps of width 5. The smoothing is demonstrated in Fig. 5b, where we show the mounds in the absence and presence of the alternating field after time $t = 10^{-6}$ s. One can see that, as expected, even in the absence of the ac field some smoothing takes place, due to the high curvature of the surface. However, as the figure demonstrates, smoothing is dramatically improved in the presence of the ac field. While the mounds would just drift in the presence of a dc field, they are smoothed by an ac field. In other words, even though the mounds have two opposite sides, the downhill current acts

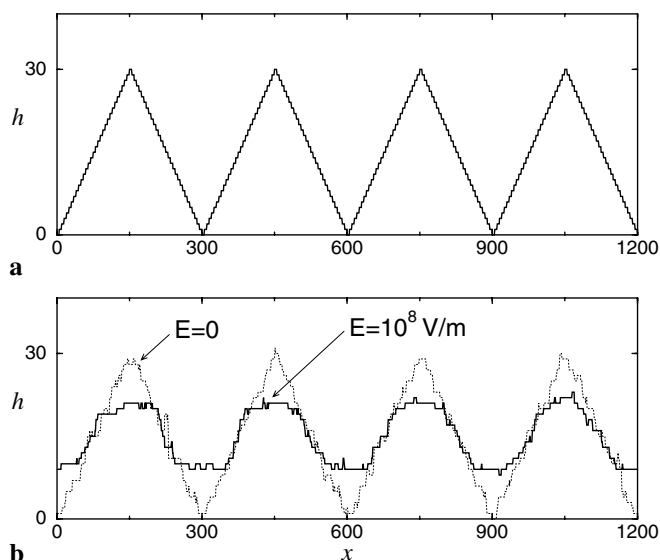


FIGURE 5 **a** The initial mound structure. **b** Comparison of the surface morphologies with and without the application of an ac field after 10^{-6} s. Parameters used: the base size of the triangular mounds is 300 lattice constants, the height is 30, $T = 500$ K, $E_0 = 0.3$ eV, $E_1 = 0.6$ eV, $E_b = 0.15$ eV, $Z = 0.5$, and $v_0 = 10^{13}$ s $^{-1}$

on both sides simultaneously, decreasing the height of the mound. Note that the ratchet effect depends quadratically on the amplitude of the electric field [34]; thus for experimentally realizable values a much longer time scale is expected for the smoothing to take place.

The smoothing phenomenon has recently been tested experimentally by Pablo et al. [61, 62]. They monitored a micrometer-sized gold stripe with scanning force microscopy under both dc and ac stressing (Fig. 6). They found that in both cases the grain size gradually increased, due to the enhanced diffusion caused by the Joule heating; however, the

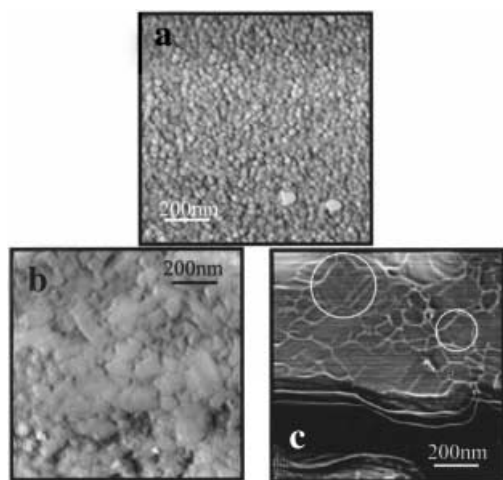


FIGURE 6 **a** Gold stripe at the very beginning of the experiment. The grain structure is clearly visible, and the grain size is about 25 nm. **b** The gold stripe after 40 h dc stressing (under a current density of 1.6×10^{11} A m $^{-2}$ with 25 mA). The grain size has grown to 100 nm. **c** Gold stripe after 24 h ac stressing (with the same rms value of the current as before). In addition to grain growth, terraces of gold can also be observed (see the marked regions, for example). The size of the images is 1 μ m \times 1 μ m. (After [61], with permission from Elsevier Science)

topographic structure of the grains was dramatically different in the two cases: for ac stressing nanometer-sized flat terraces replaced the average grains (Fig. 6c).

Since most metal and semiconductor surfaces have a non-zero Schwoebel barrier and display electromigration, we expect that the appearance of such a net current is relevant for a large class of technologically important materials. Thus, the application of an ac current during either growth or annealing can lead to a non-trivial smoothing effect and aid the growth of smooth surfaces. This consequence of the ratchet effect can thus have important practical applications in the growth and processing of high-quality thin films.

With other driving mechanisms (such as temperature oscillation or potential oscillation in an electrochemical cell) the ratchet effect can lead to the formation of surface patterns [63], providing a new tool for controlling surface morphology.

ACKNOWLEDGEMENTS I thank A.-L. Barabási, C.-S. Lee, and B. Jankó for their invaluable contributions. This work was supported by the EU Marie Curie Individual Fellowship HPMF-CT-1999-00124.

REFERENCES

- 1 M. Tinkham: *Introduction to Superconductivity* (McGraw-Hill, New York 1996)
- 2 G.B. Donaldson, C.M. Pegrum, R.J.P. Bain: In: *SQUID '85: Proc. 3rd Int. Conf. on Superconducting Quantum Devices*, ed. by H.D. Hahlbohm, H. Lübbig (Walter Gruyter, Berlin 1985) pp. 749–753
- 3 J. Clarke: In *SQUID Sensors: Fundamentals, Fabrication and Application*, ed. by H. Weinstock (Kluwer, Dordrecht 1996) pp. 1–62
- 4 D. Koelle, R. Kleiner, F. Ludwig, E. Dantsker, J. Clarke: *Rev. Mod. Phys.* **71**, 631 (1999)
- 5 G. Blatter, M.V. Feigelman, V.B. Geshkenbeim, A.I. Larkin, V.M. Vinokur: *Rev. Mod. Phys.* **66**, 1125 (1994)
- 6 R.H. Koch, J.Z. Sun, V. Foglietta, W.J. Gallagher: *Appl. Phys. Lett.* **67**, 709 (1995)
- 7 E. Dantsker, S. Tanaka, J. Clarke: *Appl. Phys. Lett.* **70**, 2037 (1997)
- 8 S. Schöne, M. Mück, C. Heiden: *Appl. Phys. Lett.* **68**, 859 (1996)
- 9 C.-S. Lee, B. Jankó, I. Derényi, A.-L. Barabási: *Nature* **400**, 337 (1999)
- 10 A. Ajdari, J. Prost: *C.R. Acad. Sci. Paris* **315**, 1635 (1992)
- 11 M.O. Magnasco: *Phys. Rev. Lett.* **71**, 1477 (1993)
- 12 R.D. Astumian, M. Bier: *Phys. Rev. Lett.* **72**, 1766 (1994)
- 13 J. Prost, J.-F. Chauwin, L. Peliti, A. Ajdari: *Phys. Rev. Lett.* **72**, 2652 (1994)
- 14 C.R. Doering, W. Horsthemke, J. Riordan: *Phys. Rev. Lett.* **72**, 2984 (1994)
- 15 R.D. Astumian: *Science* **276**, 917 (1997)
- 16 F. Jülicher, A. Ajdari, J. Prost: *Rev. Mod. Phys.* **69**, 1269 (1997)
- 17 P. Hänggi, R. Bartussek: In *Lecture Notes in Physics, Vol. 476*, ed. by J. Parisi et al. (Springer, Berlin, Heidelberg 1996) pp. 294–308
- 18 I. Derényi, T. Vicsek: In *Fluctuations and Scaling in Biology*, ed. by T. Vicsek (Oxford University Press, New York 2001) pp. 117–176
- 19 C.J. Olson, C. Reichhardt, B. Jankó, F. Nori: *Phys. Rev. Lett.* **87**, 177 002 (2001)
- 20 B.Y. Zhu, B.R. Zhao, Z.X. Zhao, L. Van Look, V.V. Moshchalkov: *Physica C* **341**, 1143 (2000)
- 21 F. Pardo, F. de la Cruz, P.L. Gammel, E. Bucher, C. Ogelsby, D.J. Bishop: *Phys. Rev. Lett.* **79**, 1369 (1997)
- 22 B.L.T. Plourde, D.J. Van Harlingen, R. Besseling, M.B.S. Hesselberth, P.H. Kess: *Physica C* **341**, 1023 (2000)
- 23 C. Reichhardt, C.J. Olson, F. Nori: *Phys. Rev. B* **58**, 6534 (1998)
- 24 C. Reichhardt, C.J. Olson, F. Nori: *Phys. Rev. Lett.* **78**, 2648 (1997)
- 25 C.J. Olson, C. Reichhardt, F. Nori: *Phys. Rev. Lett.* **81**, 3757 (1998)
- 26 E. Zeldov, A.I. Larkin, V.B. Geshkenbeim, M. Konczykowski, D. Majer, B. Khaykovich, V.M. Vinokur, H. Shtrikman: *Phys. Rev. Lett.* **73**, 1428 (1994)
- 27 J.R. Clem, R.P. Huebener, D.E. Gallus: *J. Low Temp. Phys.* **12**, 449 (1973)
- 28 M. Mück: *Superlattices Microstruct.* **21**, 415 (1997)

- 29 B.A. Scott, J.R. Kirtley, D. Walker, B.-H. Chen, Y. Wang: *Nature* **389**, 164 (1997)
- 30 J. Rousselet, L. Salome, A. Ajdari, J. Prost: *Nature* **370**, 446 (1994)
- 31 L.P. Faucheux, L.S. Bourdieu, P.D. Kaplan, A.J. Libchaber: *Phys. Rev. Lett.* **74**, 1504 (1995)
- 32 N. Konomura, R.W.J. Zijlstra, R.A. van Delden, N. Harada, B.L. Fer- inga: *Nature* **401**, 152 (1999)
- 33 T.R. Kelly, H. De Silva, R.A. Silva: *Nature* **401**, 150 (1999)
- 34 I. Derényi, C.-S. Lee, A.-L. Barabási: *Phys. Rev. Lett.* **80**, 1473 (1998)
- 35 I. Zapata, R. Bartussek, F. Sols, P. Hänggi: *Phys. Rev. Lett.* **77**, 2292 (1996)
- 36 I. Zapata, J. Luczka, F. Sols, P. Hänggi: *Phys. Rev. Lett.* **80**, 829 (1998)
- 37 S. Weiss, D. Koelle, J. Müller, R. Gross, K. Barthel: *Europhys. Lett.* **51**, 499 (2000)
- 38 F. Falo, P.J. Martinez, J.J. Mazo, S. Cilla: *Europhys. Lett.* **45**, 700 (1999)
- 39 E. Trías, J.J. Mazo, F. Falo, T.P. Orlando: *Phys. Rev. E* **61**, 2257 (2000)
- 40 E. Goldobin, A. Sterck, D. Koelle: *Phys. Rev. E* **63**, 031 111 (2001)
- 41 G. Carapella, G. Costabile, *Phys. Rev. Lett.* **87**, 077 002 (2001)
- 42 J.F. Wambaugh, C. Reichhardt, C.J. Olson, F. Marchesoni, F. Nori: *Phys. Rev. Lett.* **83**, 5106 (1999)
- 43 A. Pruyboom, P.H. Kes, E. van der Drift, S. Radelaar: *Phys. Rev. Lett.* **60**, 1430 (1988)
- 44 G.W. Slater, H.L. Guo, G.I. Nixon: *Phys. Rev. Lett.* **78**, 1170 (1997)
- 45 T.A.J. Duke R.H. Austin: *Phys. Rev. Lett.* **80**, 1552 (1998)
- 46 D. Ertas: *Phys. Rev. Lett.* **80**, 1548 (1998)
- 47 I. Derényi, R.D. Astumian: *Phys. Rev. E* **58**, 7781 (1998)
- 48 J. Villain: *J. Phys. I* **1**, 19 (1991)
- 49 M.D. Johnson, C. Orme, A.W. Hunt, D. Graff, J. Sudijono, L.M. Sander, B.G. Orr: *Phys. Rev. Lett.* **72**, 116 (1994)
- 50 J.A. Strosio, D.T. Pierce, M.D. Stiles, A. Zangwill, L.M. Lander: *Phys. Rev. Lett.* **75**, 4246 (1995)
- 51 J.-K. Zuo, J.F. Wendelken: *Phys. Rev. Lett.* **78**, 2791 (1997)
- 52 R.L. Schwoebel: *J. Appl. Phys.* **40**, 614 (1969)
- 53 S. Kodiyalam, K.E. Khor, S. Das Sarma: *Phys. Rev. B* **53**, 9913 (1996)
- 54 H. Yasunaga, A. Natori: *Surf. Sci. Rep.* **15**, 205 (1992)
- 55 M. Ichikawa, T. Doi: *Vacuum* **41**, 933 (1990)
- 56 B.H. Jo, R.W. Vook: *Appl. Surf. Sci.* **89**, 237 (1995)
- 57 P.J. Rous, T.L. Einstein, E.D. Williams: *Surf. Sci.* **315**, L995 (1994)
- 58 D. Kandel, E. Kaxiras: *Phys. Rev. Lett.* **76**, 1114 (1996)
- 59 A.H. Verbruggen: *IBM J. Res. Dev.* **32**, 93 (1988)
- 60 I. Derényi, T. Vicsek: *Phys. Rev. Lett.* **75**, 374 (1995)
- 61 P.J. Pablo, J. Colchero, J. Gómez-Herrero, A. Asenjo, M. Luna, P.A. Serena, A.M. Baró: *Surf. Sci.* **464**, 123 (2000)
- 62 P.J. Pablo, A. Asenjo, J. Colchero, P.A. Serena, J. Gómez-Herrero, A.M. Baró: *Surf. Interface Anal.* **30**, 278 (2000)
- 63 O. Pierre-Louis, M.I. Haftel: *Phys. Rev. Lett.* **87**, 048 701 (2001)